Langmuir
Article
pubs.acs.org/Langmuir

Biomagnetic Glasses: Preparation, Characterization, and Biosensor Applications

Yu-Ho Won,[†] Ho Seong Jang,[¶] Seung Min Kim,[†,‡] Eric Stach,[†,‡] Mallikarjunarao Ganesana,[§] Silvana Andreescu,[§] and Lia A. Stanciu*[,†,‡]

[†]*School of Materials Engineering, Purdue University, West Lafayette, Indiana 47907,* [‡]*Birck Nanotechnology Center, Purdue University, West Lafayette, Indiana 47907,* [§]*Department of Chemistry, Clarkson University, Potsdam, New York 13699-5810, and* [¶]*Department of Chemistry, Purdue University, West Lafayette, Indiana 47907*

Received September 10, 2009. Revised Manuscript Received October 22, 2009

In this work, a novel avenue to create a generic approach for the fabrication of biofunctional materials with magnetic capabilities to be used in the design of highly stable, magnetically separable enzyme-based systems was explored. As a model system, immobilization of acetylcholinesterase (AChE) was investigated using biomagnetic glasses composed of a magnetic core with a size tunable porous silica shell. The efficiency of the immobilization was determined by analyzing the biosensing capability of these biomagnetic glasses for the detection of the organophosphorous pesticide paraoxon. Screen printed electrodes with the AChE-biomagnetic glasses showed higher current response and stability than for the free enzyme. The detection limit of the paraoxon biosensor was in the nanomolar range.

1. Introduction

Functionalized magnetic particles have found numerous applications in the biomedical field, as well as in therapeutics, bioimaging, and biosensors areas.[1] Significant progress has been made in the control of chemical composition, size, size distribution, and shape of magnetic nanoparticles (NPs) in recent years.[2] There are several types of magnetic particles that were investigated so far. An example are those displaying an inorganic magnetic core (e.g., iron oxide), surrounded by an outer layer of silica, long-chain organic ligands, or various types of polymers. It is on this outer shell where otherwise unstable biological molecules could attach, thus providing bioactivity to such magnetic particles that could further be used in the construction of bioanalytical devices, such as biosensors. The functional properties of biomolecules make them interesting candidates for a large array of applications in fields such as medicine, defense, or energy. However, they typically have low stability at ambient temperatures, which severely limits their usability for practical applications. To overcome this problem, immobilization of the biomolecules in a functional state into an inorganic matrix can be useful for the development of bioanalytical devices. A successful bioimmobilization procedure results in a robust material, which retains the activity and functional properties of the biomolecule, while tremendously increasing its reuse potential and stability over time.[3] Enzymes can be encapsulated into or onto a material through different mechanisms: covalent binding to surfaces, physical adsorption, and entrapment in semipermeable membranes or microencapsulation into hydrogels and polymer microspheres. A good matrix for enzyme immobilization at the material's surface, in addition to being very stable, allowing for long-term storage after immobilization of the enzyme, needs to be or be modified to become reactive with chemical groups present in enzymes' structure (e.g., amine, hydroxyl, thiol). The reactivity between the matrix material and the enzymes is necessary in order for the immobilization procedure to yield very stable enzyme−matrix bonds, resulting from a multipoint enzyme−matrix covalent attachment.[4,5] In addition, any remaining reactive groups of the matrix that did not couple with the enzyme via multipoint immobilization can be blocked with various compounds to finally result in an inert enzyme−matrix hybrid material with high stability.[6] Another avenue for enzyme immobilization is through adsorption of the enzyme into the pores of a material that was applied especially for sol−gel silica materials.[7,8] The drawbacks associated with this method include difficulties with analyte diffusion to the entrapped enzyme, enzyme leaching, and enzyme orientation problems.

Magnetic beads have been used for the design of immunomagnetic electrochemical sensors through the immobilization of an antibody on the surface of an electrochemical transducer.[9−14] The utilization of reusable antibody-coated magnetic microparticles is efficient in overcoming the main problem of immunosensors,

*Corresponding author. Tel.: +1-765-496-3552. Fax: +1-765-494-1204. E-mail: lstanciu@purdue.edu.

(1) Sun, C.; Lee, J. S. H.; Zhang, M. *Adv. Drug Deliver. Rev.* **2008**, *60*, 1252–1265.
(2) (a) Yin, Y.; Alivisatos, A. P. *Nature* **2005**, *437*, 664–670. (b) Burda, C.; Chen, X. B.; Narayanan, R.; El-Sayed, M. A. *Chem. Rev.* **2005**, *105*, 1025–1102.
(3) (a) Mateo, C.; Palomo, J. M.; Fernandez-Lorente, G.; Guisan, J. M.; Fernandez-Lafuente, R. *Enzyme Microb. Technol.* **2007**, *40*, 1451–1463. (b) Iyer, P. V.; Ananthanarayan, L. *Process Biochem.* **2008**, *43*, 1019–1032.
(4) Nunes, G. S.; Montesinos, T.; Marques, P. B. O.; Fournier, D.; Marty, J.-L. *Anal. Chim. Acta* **2001**, *434*, 1–7.
(5) Albareda-Sirvent, M.; Merkoci, A.; Alergret, S. *Sens. Actuators B* **2000**, *60*, 153–158.
(6) Mateo, C.; Fernandez-Lorente, G.; Cortes, E.; Garcia, J. L.; Fernandez-Lafuente, R.; Guisan, J. M. *Biotechnol. Bioeng.* **2001**, *76*, 269–276.
(7) Gill, I. *Chem. Mater.* **2001**, *13*, 3404–3421.
(8) Jin, W.; Brennan, J. D. *Anal. Chim. Acta* **2002**, *461*, 1–36.
(9) (a) Santandreu, M.; Sole, S.; Fabregas, E.; Alegret, S. *Biosens. Bioelectron.* **1998**, *13*, 7–17. (b) Sole, S.; Alegret, S.; Cespedes, F.; Fabregas, E. *Anal. Chem.* **1998**, *70*, 1462–1467.
(10) Gehring, A. G.; Brewster, J. D.; Irwin, P. L.; Tu, S. I.; Van Houten, L. J. *J. Electroanal. Chem.* **1999**, *469*, 27–33.
(11) Dequaire, M.; Degrand, C.; Limoges, B. *Anal. Chem.* **1999**, *71*, 2571–2577.
(12) Liu, Z. M.; Yang, H. F.; Li, Y. F.; Liu, Y. L.; Shen, G. L.; Yu, R. Q. *Sens. Actuator B-Chem.* **2006**, *113*, 956–962.
(13) (a) Kim, G. H.; Rand, A. G.; Letcher, S. V. *Biosens. Bioelectron.* **2003**, *18*, 83–89. (b) Kim, G. H.; Rand, A. G.; Letcher, S. V. *Biosens. Bioelectron.* **2003**, *18*, 91–99.
(14) (a) Palacek, E.; Fojta, M.; Jelen, F. *Bioelectrochemistry* **2002**, *56*, 85–90. (b) Wang, J.; Kawde, A. N.; Erdem, A.; Salazar, M. *Analyst* **2001**, *126*, 2020–2024. (c) Kerman, K.; Matsubara, Y.; Morita, Y.; Takamura, Y. *Sci. Technol. Adv. Mater.* **2004**, *5*, 351–357.

namely the need of regeneration of the sensing surface. Overcoming this problem would consist in a solution for integration of immunosensors into automatic systems, difficult to achieve otherwise due to the difficulties in renewing the sensing surface. Different analyses were detected this way, such as Rabbit IgG,[9] *E. coli*,[10] 2,4-D-herbicide,[11] Human IgG,[12] or Salmonella typhinium.[13] Another type of sensors that use magnetic microbeads is the DNA hybridization sensors.[14] With a final goal of integration in another class of biosensors, for instance, enzymatic biosensors, a variety of enzymes have been immobilized in sol−gel glasses with partial retention of enzymatic activity. However, there are still challenges, such as limited sensitivity, long response time, and non-renewability of their surface, that are associated with these types of materials. Enzymatic biosensors based on magnetic particles were also designed with advantages of offering a high specific surface area, a good environment for retention of the bioactivity, good control of the localization of the sensitive material through the use of permanent magnets that allow for the enzymatic reactions to occur close to the transducer, and the renewability of the sensitive transducer. However, there are very few reports in literature for using magnetic particles for enzymatic biosensor design. Some examples of such biosensing devices include tyrosinase for the detection of phenol,[15] yeast (YADH/NAD^+)[16] for the detection of ethanol, and glucose oxidase for glucose detection.[17] Most of these systems are based on bare magnetic particles onto which enzymes are physically absorbed or covalently linked. Preparation of core/shell enzyme−silica modified magnetic NPs and a systematic investigation of the synthetic conditions in relation to the biological activity of an immobilized enzyme, and their application to the construction of enzyme biosensors, to our knowledge, has not been reported.

Over the past decade, biosensors based on acetylcholinesterase (AChE) have emerged as a promising technique for toxicity analysis, environmental monitoring, food quality control, and military investigations.[18,19] The main application of AChE biosensors is for the detection of organophosphate and carbamate pesticides based on enzyme inhibition. Fabrication of AChE biosensors involves immobilization of the AChE enzyme onto an electrode surface. Various immobilization strategies and materials have been used for this purpose including physical and covalent binding and affinity interactions. One attractive method that ensures stability of the enzymatic layer is to entrap the enzyme in a silica material prepared by low temperature sol−gel processing. A variety of enzymes, including AChE have been immobilized in silica sol−gel glasses with retention of enzymatic activity.[20] Several reports demonstrated the possibility of combining sol−gel technology with screen-printing protocols for biosensor fabrication.[21,22] Other reports have indicated the potential of the sol−gel method as a versatile and efficient technique for conserving enzyme activity in organic solvents.[22,23] Studies have demonstrated that immobilization in a sol−gel material requires lower enzyme loading as compared to covalent binding via glutaraldehyde to obtain comparable current values.[24] Andreescu et al. used this method to immobilize genetically modified AChE onto screen printed electrodes (SPEs) and reported an enhanced enzymatic stability.[25] However, there are several drawbacks of using silica gels for enzyme immobilization, such as brittleness, a poor orientation of the enzyme, nonrenewability of the sensing surface, and an aggressive chemical environment that can lead to enzyme denaturation and negatively impact the sensor performance.

Recently, a large number of enzyme immobilization based on the core/shell structured materials have been developed. Deng et al. reported colloidal magnetic zeolite microspheres for the immobilization of trypsin.[26] Zheng et al. synthesized CdSe/ZnS core/shell quantum dots and used them in biosensors.[27] Cai et al. prepared $Au/CaCO_3$ hybrid materials for the immobilization of horseradish peroxidase (HPR) enzyme.[28] More recently, silica/iron oxide nanocomposites were reported for enzyme immobilization.[29] However, the nanocomposites were agglomerated and the silica shell was not uniform, making it difficult to achieve a desired high surface area of nanocomposites for enzyme immobilization.

Here, we report on the synthesis and characterization of novel hybrid biomagnetic nanocomposites, called biomagnetic glasses, consisting of an inorganic core (Fe_3O_4 NPs), a mesoporous silica shell, and a model enzyme (AChE). To test the capability of these materials to serve as a platform for enzyme immobilization, AChE was selected as a model enzyme. Fe_3O_4 NPs/mesoporous silica core/shell nanocomposites (Fe_3O_4/m-silica, unless noted, Fe_3O_4/m-silica represents Fe_3O_4 NPs/ mesoporous silica core/shell nanocomposites) were used to immobilize AChE to fabricate a biosensor for the detection of the pesticide paraoxon as an example of potential application of these materials.

2. Experimental Section

Chemicals. Iron chloride ($FeCl_3 \cdot 6H_2O$), sodium oleate, oleic acid, 1-octadecene, tetraethyl orthosilicate (TEOS), ammonium hydroxide, sodium dodecyl sulfate (SDS), IGEPAL CO-520 and hexane were purchased from Sigma Aldrich for synthesis of Fe_3O_4 NPs and Fe_3O_4/mesoporous silica (m-silica) core/shell nanocomposites. Acetylcholinesterase (AChE), acetylthiocholine chloride (ATChCl), phosphate buffered saline (PBS), 5,5′-dithio-(2-nitrobenzoic acid) (DTNB), and paraoxon were obtained from Sigma Aldrich for detection of paraoxon. All chemicals were of reagent grade.

(15) Liu, Z.; Liu, Y.; Yang, H.; Yang, Y.; Shen, G.; Yu, R. *Anal. Chim. Acta* **2005**, *533*, 3–9.
(16) Ivanova, V.; Hristov, J.; Dobreva, E.; Al-Hassan, Z.; Penchev, I. *Appl. Biochem. Biotechnol.* **1996**, *59*, 187–198.
(17) (a) Njagi, J.; Andreescu, S. *Biosens. Bioelectron.* **2007**, *23*, 168–175. (b) Andreescu, S.; Njagi, J.; Ispas, C. In *The New Frontiers of Organic and Composite Nanotechnology*; Erokhin, V., Ram, M. K., Yavuz, O., Eds.; Elsevier: Amsterdam, Netherlands, 2007; Chapter 7.
(18) (a) Fest, C.; Schmidt, K. In *The Chemistry of Organophosphorus Pesticides, Reactivity, Synthesis, Mode of Action, Toxicology*; Fest, C., Schmidt, K., Eds.; Springer: Heidelberg, NY, 1973. (b) Hosea, N. A.; Berman, H. A.; Taylor, P. *Biochemistry* **1995**, *34*, 11528–11536.
(19) Andreescu, S.; Marty, J. L. *Biomol. Eng.* **2006**, *23*, 1–15.
(20) (a) Gill, I.; Ballesteros, A. *Trends Biotechnol.* **2000**, *18*, 282–296. (b) Kandimalla, V. B.; Tripathi, V. S.; Ju, H. X. *Crit. Rev. Anal. Chem.* **2006**, *36*, 73–106. (c) Sotiropoulou, S.; Chaniotakis, N. A. *Biomaterials* **2005**, *26*, 6771–6779. (d) Anitha, K.; Mohan, S. V.; Reddy, S. J. *Biosens. Bioelectron.* **2004**, *20*, 848–856. (e) Niu, J. J.; Lee, J. Y. *Sens. Actuator B-Chem.* **2002**, *82*, 250–258. (f) Wang, B.; Zhang, J.; Dong, S. *Biosens. Bioelectron.* **2000**, *15*, 397–402. (g) Tsai, H. C.; Doong, R. A. *Water Sci. Technol.* **2000**, *42*, 283. (h) Wang, J. *Analy. Chim. Acta* **1999**, *399*, 21–27. (i) Iwuoha, E. I.; Kane, S.; Ania, C. O.; Smyth, M. R.; Montellano, P. R. O.; Fuhr, U. *Electroanalysis* **2000**, *12*, 980–986. (j) Maurer, S. C.; Schulze, H.; Schmid, R. D.; Urlacher, V. *Adv. Synth. Catal.* **2003**, *345*, 802–810.
(21) Albareda-Sirvent, M.; Hart, A. L. *Sens. Actuator B-Chem.* **2002**, *87*, 73–81.
(22) Wang, J.; Pamidi, P. V. A.; Park, D. S. *Anal. Chem.* **1996**, *68*, 2705–2708.
(23) (a) Vidinha, P.; Augusto, V.; Almeida, M.; Fonseca, I.; Fidalgo, A.; Ilharco, L.; Cabral, J. M. S.; Barreiros, S. *J. Biotechnol.* **2006**, *121*, 23–33. (b) Yu, J. H.; Ju, H. X. *Electroanalysis* **2004**, *16*, 1305–1310. (c) Wang, B. Q.; Dong, S. J. *J. Electroanal. Chem.* **2000**, *487*, 45–50. (d) Adanyi, N.; Toth-Markus, M.; Szabo, E. E.; Varadi, M.; Sammartino, M. P.; Tomassetti, M.; Campanella, L. *Anal. Chim. Acta* **2004**, *501*, 219–225.
(24) Nunes, G. S.; Jeanty, G.; Marty, J. L. *Anal. Chim. Acta* **2004**, *523*, 107–115.
(25) Andreescu, S.; Barthelmebs, L.; Marty, J. L. *Anal. Chim. Acta* **2002**, *464*, 171–180.
(26) Deng, Y.; Deng, C.; Qi, D.; Liu, C.; Liu, J.; Zhang, X.; Zhao, D. *Adv. Mater.* **2009**, *21*, 1377–1382.
(27) Ji, X.; Zheng, J.; Xu, J.; Rastogi, V. K.; Cheng, T. −C.; DeFrank, J. J.; Leblanc, R. M. *J. Phys. Chem. B* **2005**, *109*, 3793–3799.
(28) Cai, W. −Y.; Xu, Q.; Zhao, X. −N.; Zhu, J. −J.; Chen, H. −Y. *Chem. Mater.* **2006**, *18*, 279–284.
(29) (a) Shukoor, M. I.; Natalio, F.; Therese, H. A.; Tahir, M. N.; Ksenofontov, V.; Panthofer, M.; Eberhardt, M.; Theato, P.; Schroder, H. C.; Muller, W. E. G.; Tremel, W. *Chem. Mater.* **2008**, *20*, 3567–3573. (b) Valdes-Solis, T.; Rebolledo, A. F.; Sevilla, M.; Valle-Vigon, P.; Bomati-Miguel, O.; Fuertes, A. B.; Tartaj, P. *Chem. Mater.* **2009**, *21*, 1806–1814.

Scheme 1. Synthesis Procedure of Fe_3O_4/m-Silica and the Electrochemical Cell Setup Using Enzyme Immobilized Hybrid Nanocomposites

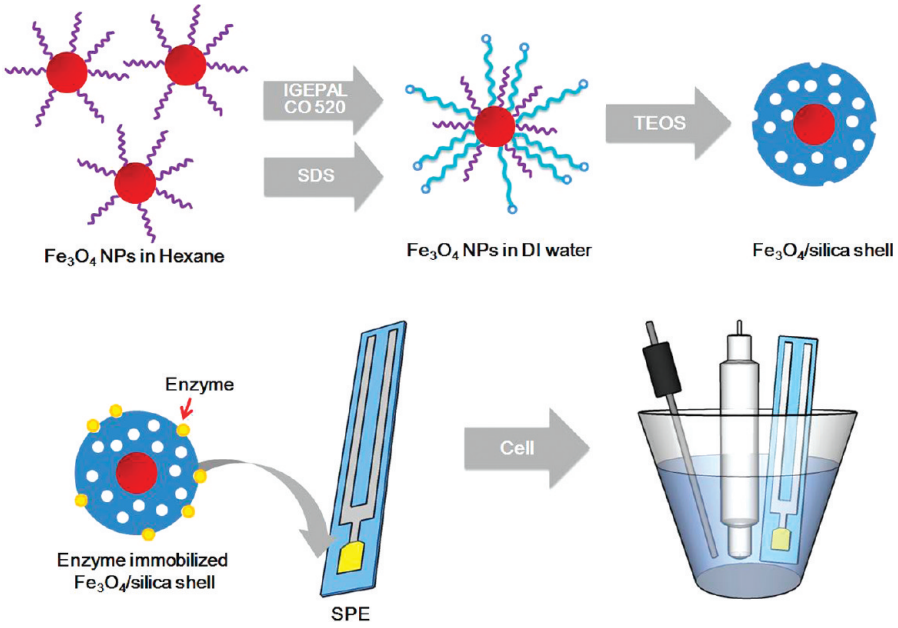

Synthesis of Fe_3O_4 NPs. Fe_3O_4 NPs were prepared via the synthesis method proposed by Park et al.[30] An iron-oleate complex was synthesized from 0.54 g of iron chloride and 1.83 g of sodium oleate. The solution including two chemicals and the mixed solvent of 3.5 mL of ethanol, 3.0 mL of deionized (DI) water, and 7.0 mL of hexane was heated to 70 °C for 4 h. After the reaction, the solution was washed with DI water and dried. The iron-oleate (1.8 g), oleic acid (0.29 g), and 1-octadecene (10 g) were prepared in a three-neck flask, and the solution was heated to 320 °C for 30 min. The resulting solution was then cooled to room temperature by adding hexane, and enough ethanol was added to precipitate the NPs. Finally the Fe_3O_4 NPs were dispersed in hexane after several times of washing and centrifugation.

Synthesis of Fe_3O_4/m-Silica Nanocomposites. The core/shell nanocomposites were synthesized by the method proposed by Yi et al.[31] IGEPAL CO-520 (0.6 mL) was added in the solution including the synthesized Fe_3O_4 NPs (1.0 mL) and hexane (11.25 mL). The solution was sonicated to disperse IGEPAL CO-520 for 10 min. A 0.10 mL portion of ammonium hydroxide was added to the solution. Then, TEOS (0.3 mL for the silica shell with 20 nm thickness) was added, and the mixture was vortexed for about 20 h. The resulting solution was washed and centrifuged. At last, the Fe_3O_4/m-silica particles were dispersed in DI water.

Preparation of Electrodes. The AChE solution was prepared in PBS (pH 7.4), and the substrate solution, ATChCl, was prepared in 0.9 wt % NaCl solution. The concentration of AChE was measured by Ellman's assay.[32] Briefly, 100 μL of AChE solution with 3.53 mU enzyme was added into 100 μL of Fe_3O_4/m-silica solution. The AChE immobilized Fe_3O_4/m-silica were deposited on screen printed electrodes (SPE) obtained from Pine Research Instrumentation. The SPE were dried in air for 2 h at room temperature and then stored in PBS at 4 °C before use. The electrochemical cell was set up with 3 mL PBS and three electrodes: SPE (working electrode), Ag/AgCl reference electrode, and Pt wire auxiliary electrode

Characterization. Transmission electron microscopy (TEM) images of the synthesized Fe_3O_4 NPs and Fe_3O_4/m-silica were observed using Titan 80-300 and Tecnai 20 (FEI Company, USA) transmission electrode microscopes, operated at 300 and 200 kV, respectively. Scanning electron microscopy (SEM) images of the nanocomposites were obtained using an FEI Nova NanoSEM 200 operated at 10 kV. The X-ray diffraction patterns of the nanocomposites were measured with a Bruker D8 focus (Cu Kα raditation, λ = 1.5406 Å). The ultraviolet−visible (UV−vis) spectroscopy was recorded using SpectraMax M5 spectrometer from Molecular devices in order to measure AChE concentration. The current response of the fabricated SPEs was measured using BASi epsilon C3 cell stand.

Electrochemical Measurements and Determination Procedures. All electrochemical measurements were carried out with the AChE-modified SPE immersed in a cell containing 3 mL of PBS solution at pH 7.4. Amperometric measurements were used to characterize the fabricated pesticide biosensor. For amperometric measurements, the electrochemical cell was stirred with a mechanical stirrer (IKA R103 Stand). Measurements were carried out at fixed applied potential of 235 mV vs Ag/AgCl screen-printed pseudoreference electrode. After stabilization of the capacitive current, the enzymatic reaction was initiated by the addition of 1.0 mM ATChCl substrate and the response of the sensor was measured. The operational stability of the biosensor was evaluated by measuring repetitively the electrode response to the same quantity of ATChCl substrate (final concentration 1.0 mM) and rinsing the cell between measurements. The storage stability was evaluated by measuring the response of electrodes, stored under the same conditions, at various time intervals. The reproducibility was evaluated from the response of identically prepared electrodes. Inhibition measurements were carried out in a two-step batch procedure[24] by measuring the response of the sensor to additions of a constant amount of ATChCl substrate (1.0 mM) before and after inhibition with pesticides. All inhibition measurements were carried out with paraoxon as a model organophosphate pesticide. The electrodes were incubated for 10 min in DI water in the absence and presence of concentrations of paraoxon ranging from 10^{-9} to 10^{-5} M.

3. Results and Discussion

3.1. Synthesis of the Biomagnetic Glasses. The results of this work demonstrate a significant capacity of our synthesized biomagnetic glasses to serve as a biosensor platform for the detection of pesticides following the induction of their catalytic

(30) Park, J.; An, K.; Hwang, Y.; Park, J.-G.; Noh, H.-J.; Kim, J.-Y.; Park, J.-H.; Hwnag, N.-M.; Hyeon, T. *Nat. Mater.* **2004**, *3*, 891–895.
(31) Yi, D. K.; Selvan, S. T.; Lee, S. S.; Papaefthymiou, G. C.; Kundaliya, D.; Ying, J. Y. *J. Am. Chem. Soc.* **2005**, *127*, 4990–4991.
(32) Ellman, G. L.; Courtney, K. D.; Andres, V.; Featherstone, R. M. *Biochem. Pharmacol.* **1961**, *7*, 88–95.

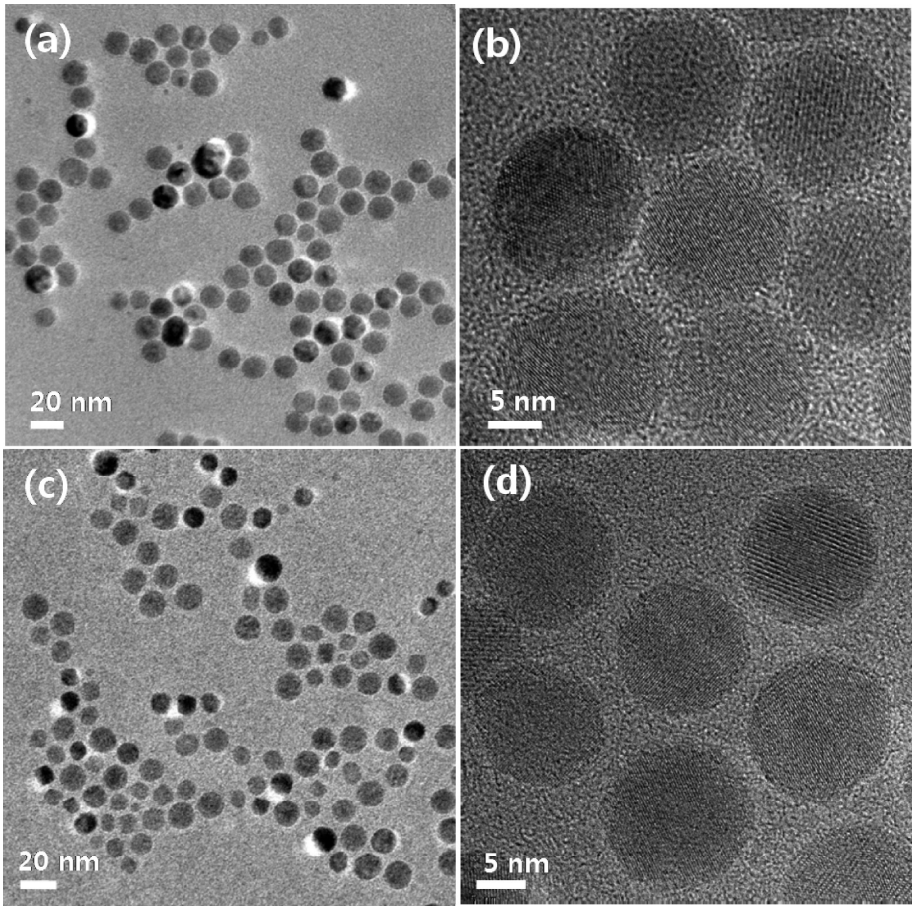

Figure 1. TEM images of 13 nm Fe_3O_4 NPs (a) dispersed in hexane, (b) the high-resolution image of (a), (c) dispersed in DI water, and (d) the high-resolution image of (c).

properties through immobilization of AChE on their surface, exposure to the acetylthiocholine chloride (ATChCl) substrate, and electrochemical detection. Scheme 1 lays out the details of the synthesis method used for the formation of enzyme containing biomagnetic glasses. The synthesized Fe_3O_4 NPs are initially hydrophobic. We employed a method using two different surfactants IGEPAL CO-520 or sodium dodecyl suflate (SDS) to generate and enhance the hydrophilic surface property of the iron oxide NPs that were initially dispersed in hexane. Since coating with a mesoporous silica shell is expected to lead to better results for enzyme immobilization than the bare magnetic NPs, this layer was fabricated around the Fe_3O_4 core. The ultimate goal of our synthesis steps shown in Scheme 1 was to use the biomagnetic glasses for AChE immobilization on their surface and electrochemical detection of paraoxon. The electrochemical cell was set up with three electrodes: a Pt wire auxiliary electrode, an Ag/AgCl reference electrode, and a working electrode.

3.2. Characterization of Biomagnetic Glasses. The monodispersity and high crystallinity of the bare Fe_3O_4 NPs dispersed in hexane were confirmed by transmission electron microscopy (TEM) analysis (Figure 1). The particle size of the NPs in Figure 1a,b was measured to be of 13 nm in diameter. Figure 1b reveals a phase contrast high-resolution TEM image of the Fe_3O_4 NPs. The lattice fringes in Figure 1b are indicative of a high crystallinity of the NPs. Figures 1c and 1d reveal that after surface modification to hydrophilic by SDS and dispersion in DI water, the NPs are still very well dispersed, with no agglomeration and that they maintain their crystallinity. The TEM results show

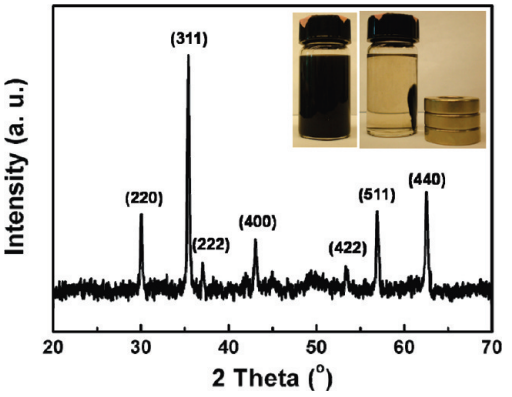

Figure 2. XRD pattern of Fe_3O_4 NPs and pictures showing magnetic properties of Fe_3O_4 NPs (inset).

that the bare Fe_3O_4 NPs are uniform in size and morphology and can be well dispersed in both hydrophobic and hydrophilic solvents by a simple surface modification procedure.

X-ray diffraction (XRD) experiments were performed to distinguish between different possible iron oxide phases (Fe_2O_3, Fe_3O_4, or FeO). Figure 2 shows the XRD pattern of as-synthesized Fe_3O_4 NPs. By comparison with JCPDS No. 75-0033, all peaks in the pattern could be indexed to magnetite (Fe_3O_4). To test the hypothesis that the Fe_3O_4 NPs were magnetic, we placed a permanent magnet near a solution of these particles (Figure 2, inset). It appears from the figure that when a magnet was placed near the glass vial, the black NPs were attracted toward it.

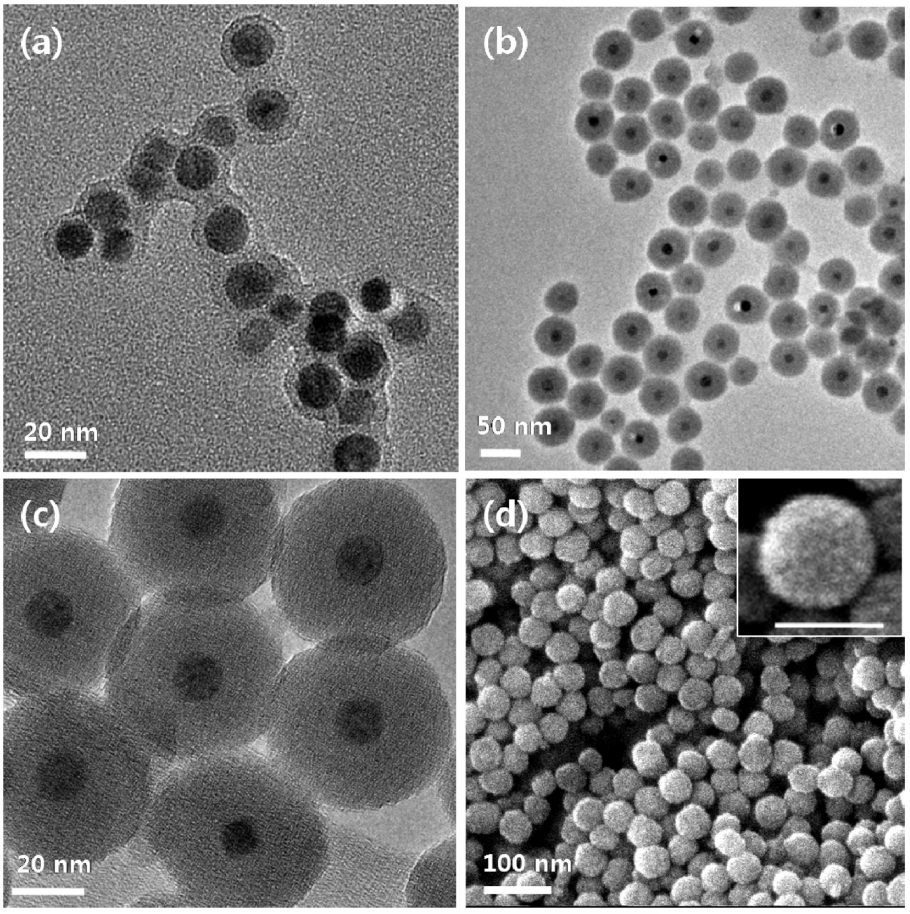

Figure 3. TEM images of (a,b) Fe_3O_4/m-silica with 13 nm Fe_3O_4 core, and 5 and 20 nm silica shell, respectively, (c) TEM image at high magnification of panel b, and (d) SEM image of Fe_3O_4/m-silica (the scale bar of the inset is 50 nm).

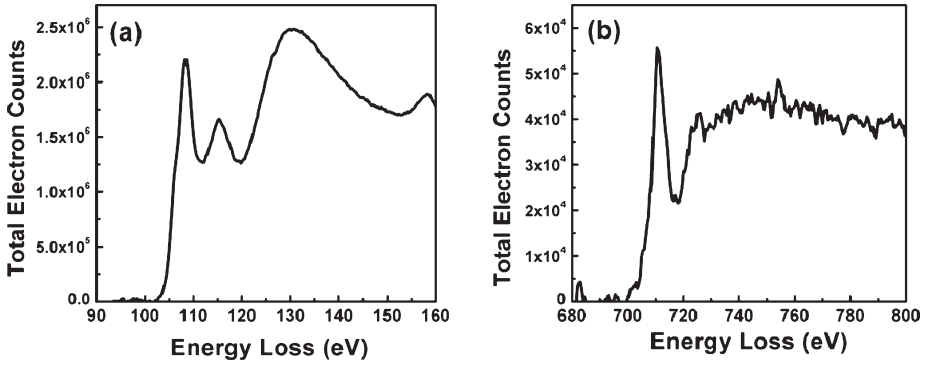

Figure 4. Electron energy loss spectra from the Fe_3O_4/m-silica. The spectra show (a) the Si-$L_{2,3}$ of SiO_2 and (b) the Fe-$L_{2,3}$ of Fe_3O_4, after background subtraction.

A mesoporous silica shell was fabricated around the core Fe_3O_4 NPs by a reverse microemulsion approach.[31,33] Ammonium hydroxide (NH_4OH) and TEOS were used as catalyst and precursor, respectively. The resulting Fe_3O_4/m-silica particles were dispersed in DI water, as required for biological applications. TEM analysis was also performed to characterize these core/shell nanocomposites for size and general microstructure (Figure 3). The results reveal that indeed these nanocomposites are very uniform in particle size and thickness of the mesoporous silica shell and are well dispersed in water, with no agglomeration. The results of the TEM investigation reveal that that the thickness of the silica shell can be tuned by adjusting the precursor concentration. Figure 3 panels a and b show two examples of adjusting the thickness of the silica shell, resulting in its size being changed from 5 to 20 nm, by changing the TEOS concentration from 10 to 20 mM. Figure 3c is a high magnification image of the silica shell, showing its uniformity in size and morphology. Scanning electron microscopy (SEM) imaging of the Fe_3O_4/m-silica was also performed (Figure 3d). The results show that the Fe_3O_4/m-silica are monodisperse and mesoporous.

Electron energy loss spectroscopy (EELS) was used to confirm the presence of Fe_3O_4 and SiO_2 in Fe_3O_4/m-silica. Clear Si-$L_{2,3}$ edges were observed, indicating the presence of silicon oxides (Figure 4a) at 108 and 115 eV, related to 2p → p* and 2p → d*

(33) Lu, Y.; Yin, Y.; Mayers, B. T.; Xia, Y. *Nano Lett.* **2002**, *2*, 183–186.

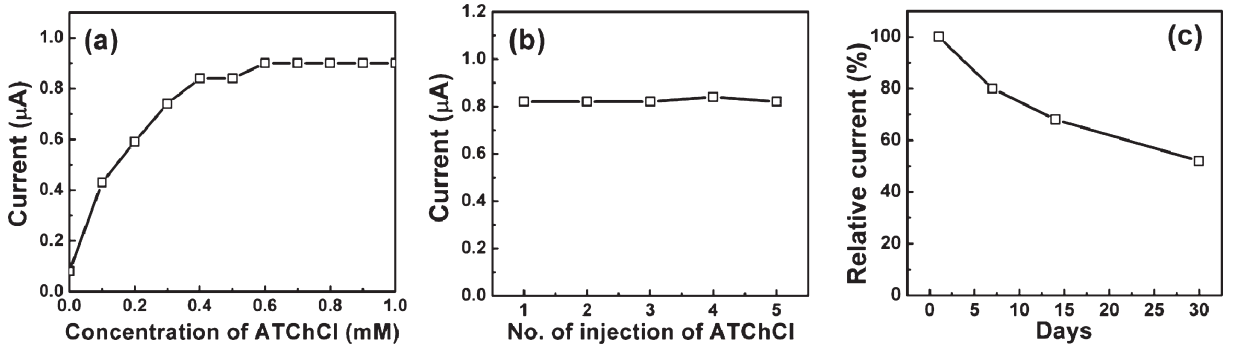

Figure 5. (a) The calibration curves of the SPEs with AChE-Fe_3O_4/m-silica; (b,c) the stability of repeated measurements and storages, respectively.

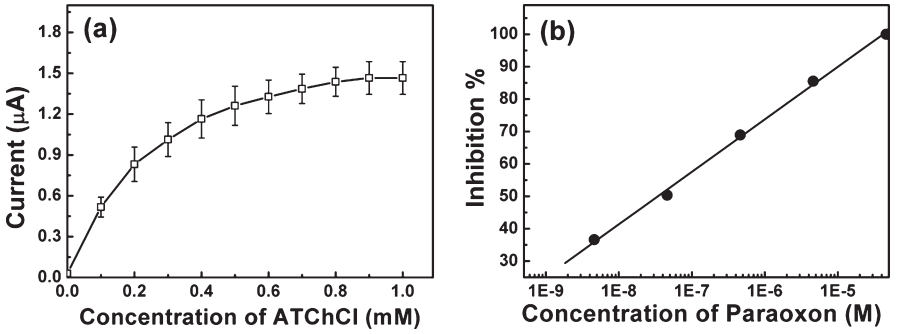

Figure 6. (a) The calibration curve of electrodes for inhibition and (b) the inhibition curve of paraoxon by using AChE-Fe_3O_4/m-silica.

transitions.[34] The Fe-L_3 and Fe-L_2 edges (background subtracted) of Fe_3O_4 in Figure 4b are observed at 711 and 723 eV, respectively.[35]

3.3. Fabrication and Electrochemical Characterization of the Paraoxon Biosensor. AChE enzyme was immobilized onto the surface of the Fe_3O_4/m-silica. Although the surface of the nanoparticles is mesoporous, the size of the pores is of about 3 nm, while the size of AChE is about 6 nm. Therefore, while some AChE molecules could partially fit into the pores, others are most likely to attach to the surface of the nanoparticles through adsorption and hydrogen bonding between the amino groups of the AChE and the free −OH groups of the silica. While using a silica layer leaves generous room for chemical modification with active groups that have the potential to enhance the stability of the hybrid system, the immobilization procedure presented here is the simplest immobilization procedure that nevertheless shows the potential of the synthesized biomagnetic glasses for applications in biosening. To further test their potential for applications in the design of enzymatic biosensors, the core−shell nanoparticles modified with enzyme through the simplest immobilization procedure, were applied to the fabrication of an amperometric biosensor to detect the pesticide paraoxon. Amperometric AChE-based biosensors generally use ATChCl as a substrate and the current response of its hydrolysis reaction under AChE catalysis is measured:

$$\text{ATChCl (substrate)} + H_2O \xrightarrow{\text{AChE (enzyme)}} \text{thiocholine (TCh)} + \text{acetate} \quad (1)$$

The AChE hydrolyzes its natural substrate, ATChCl, to TCh and acetate.[18,32] AChE is required to be stabilized for long time operation or storage because AChE, like many other enzymes, is active and moderately stable in free form and cannot fulfill its biological function. An ideal biocatalytic system requires stability under optimal reaction conditions, high activity and selectivity for the desired reaction, and minimal side reactions. The use of soluble enzymes is costly and does not allow continuous operation and reuse. Moreover, free enzymes are generally unstable, and the substrate and product cannot be easily removed from the reaction medium. A solution to these problems is through immobilization on/within inorganic materials. Before the immobilization of AChE into the nanocomposite, the concentration of AChE was obtained by ultraviolet−visible (UV−vis) spectroscopy, which was conducted at 412 nm by monitoring the formation of thionitrobenzoate, the reaction product of the reaction between 5,5′-dithio-(2-nitrobenzoic acid) (DTNB) and TCh, the product of the enzymatic hydrolysis of AChE substrate.[32] After measuring the absorption, the concentration of enzyme was calculated by using the equation proposed by Ellman et al.[32] The SPEs were prepared by the following procedure. At first, the AChE which was prepared in PBS solution (0.01 M, pH = 7.4) was immobilized into Fe_3O_4/m-silica. The obtained AChE-Fe_3O_4/m-silica were stored at 4 °C before use. Next, the AChE-Fe_3O_4/m-silica were deposited on the surface of screen printed electrodes (SPE). The SPEs were then allowed to dry at room temperature and subsequently stored in PBS at 4 °C. Figure 5 shows a comparison in the current response stabilities between the AChE-Fe_3O_4/m-silica biomagnetic glasses and free AChE. The calibration curves were measured to find the optimum concentration of the substrate as shown in Figure 5a. 1.0 mM of ATChCl was selected as an optimum concentration at which the current response was fully saturated and used for the following tests. The biomagnetic glasses (0.82 μA) displayed a catalytic activity that was about 5.5 times higher than that of the free AChE (0.15 μA). This higher catalytic activity appeared to be attributed to the localization of the enzyme by immobilization using remarkably uniform

(34) Pippel, E.; Lichtenberger, O.; Woltersdorf, J. *J. Mater. Sci. Lett.* **2000**, *19*, 2059–2060.
(35) Liu, Z. Q.; Hashimoto, H.; Song, M.; Mitsuishi, K.; Furuya, K. *Acta Mater.* **2004**, *52*, 1669–1674.

nanocomposites synthesized in this study. In addition, the short and long-term stability of the SPEs was investigated. When the current responses of SPEs were measured five times successively for the short-term reproducibility test, SPEs with the AChE immobilized Fe_3O_4/m-silica (AChE-Fe_3O_4/m-silica) showed 2% variation in current response (Figure 5). The biomagnetic glasses maintained more than 50% of their enzymatic activity after 30 days.

To determine paraoxon, the initial electrode response, in the absence of the inhibitor was determined. The electrodes were then immersed in an aqueous solution containing paraoxon at a given concentration and incubated for a fixed amount of time (10 min), and the response was measured again. The average percentage of AChE inhibition was calculated and plotted against paraoxon concentration. The concentration of AChE active sites decreases after incubation with pesticides. The concentration of paraoxon is quantified by measuring the AChE inhibition response:

$$\text{inhibition } (\%) = 100 \frac{\text{initial current} - \text{final current}}{\text{initial current}} \quad (2)$$

Figure 6a shows the calibration curve measured for seven SPEs. The standard deviation was about 12% at the saturation point, ATChCl 1.0 mM. Figure 6b shows the inhibition curve on the biosensor based on the AChE-Fe_3O_4/m-silica incubated for 10 min with different concentrations of paraoxon. The detection limit of the biosensor was about 5.0×10^{-9} M of paraoxon, or approximately 0.014 ppm. This is relevant since current EPA standards for organophosphate pesticides in the US are ranging from 0.1 to 1 ppm. Following the similar fabrication schemes, a large array of biosensors could be fabricated, including but not limited to biosensors for other organophosphate pesticides.

4. Conclusions

This study reports on the use of a novel platform, that is, biomagnetic glasses based on an iron oxide/silica/AChE composition, for the fabrication of a paraoxon biosensor. The biomagnetic glasses were fabricated by immobilization of AChE onto the surface of core/shell NPs with further deposition on disposable SPE electrodes. The core/shell NPs were monodisperse, dispersible in water. The immobilization process was performed at a neutral pH, and the results show a good electrode performance in terms of stability, reproducibility, enzyme amount, and current response. The tested platform offered the possibility to operate the biosensor at a lower overpotential (235 mV) than that reported with other electrode materials, in the absence of electrochemical mediators, and provided an effective method for stable attachment of the AChE enzyme via strong electrostatic interactions. The paraoxon biosensor displayed good operational stability, good reproducibility, and retained enzymatic activity when tested after one month. The detection limit for paraoxon was found to be in the nanomolar range. In summary, we showed that magnetic core/shell particles (Fe_3O_4/m-Silica) have the potential to serve as an alternative enzyme immobilization platform for biosensor design.

Acknowledgment. The authors are grateful for the financial support provided by NSF DMR No. 0804464 and NSF OISE No. 0728130 awards.

Supporting Information Available: Optimization data of experimental variables for the biosensor test. This material is available free of charge via the Internet at http://pubs.acs.org.